

The f -divergence and Loss Functions in ROC Curve

Song Liu (song.liu@bristol.ac.uk)
<https://allmodelsarewrong.net>
 School of Mathematics
 University of Bristol, UK

Abstract

Given two data distributions and a test score function, the Receiver Operating Characteristic (ROC) curve shows how well such a score separates two distributions. However, can the ROC curve be used as a measure of discrepancy between two distributions? This paper shows that when the data likelihood ratio is used as the test score, the arc length of the ROC curve gives rise to a novel f -divergence measuring the differences between two data distributions. Approximating this arc length using a variational objective and empirical samples leads to empirical risk minimization with previously unknown loss functions. We provide a Lagrangian dual objective and introduce kernel models into the estimation problem. We study the non-parametric convergence rate of this estimator and show under mild smoothness conditions of the real arctangent density ratio function, the rate of convergence is $O_p(n^{-\beta/4})$ ($\beta \in (0, 1]$ depends on the smoothness).

1 INTRODUCTION

The study of Receiver operating characteristic (ROC) curves has a long history in medicine (Lusted, 1971), psychology (Green and Swets, 1966) and radiology (Goodenough et al., 1974). In earlier works, the ROC curve has been primarily used to analyze the performance of different classification algorithms. An interesting trend in recent years is that the ROC curve has also been used in applications that compares two distributions, such as analyzing the mode collapsing issue of Generative Adversarial nets (GAN) (Lin et al., 2018) and diagnosing the performance amortized Markov chain Monte Carlo (Hermans et al., 2020). In both cases, authors use the ROC curve as a metric for evaluating how the generated samples resemble existing samples from the other dataset.

However, is the ROC curve a valid tool for measuring the discrepancies between two distributions given two sets of samples? Binary classification is slightly different from comparing samples from two distributions. If the ROC curve indeed reflects the differences between two distributions, how is such information encoded in the geometry of the ROC curve? Can we quantitatively measure this geometry using two sets of samples? These are the questions motivated this research.

Difference between two distributions are usually measured by various statistical divergences/distances such as Kullback-Leibler divergence Kullback and Leibler (1951) or Total Variational distance. Lately, researchers have shown an increasing interest in developing discrepancy measures (such as f -divergences (Nowozin et al., 2016), Maximum Mean Discrepancy (Gretton et al., 2012) and Optimal Transport Distance (Peyre and Cuturi, 2019)) and efficient computational methods to approximate these measures. These approximating discrepancy measures have a wide range of applications such as change detection (Liu et al., 2013), GAN (Goodfellow et al., 2014) and Variational Inference (Blei et al., 2017).

It is natural to wonder, is the ROC curve in any way related to some statistical divergences/distances? One of the most frequently used performance metric derived from the ROC geometry is Area Under the Curve (AUC). In binary classification tasks, a large AUC value generally indicates the underlying test score can separate positive and negative samples well. Can AUC become an f -divergence between positive and negative densities given some test score function? An earlier investigation (Reid and Williamson, 2011)

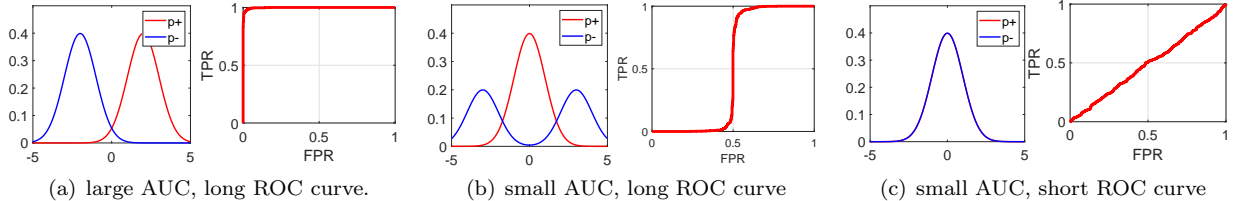


Figure 1: ROC curves generated for one dimensional datasets.

proves that the answer is no when the test score is the ratio between positive and negative data density (i.e., the likelihood ratio). Nonetheless, this result inspired us to look for f -divergence from other geometries of the ROC curve.

In this paper, we show that, when using the likelihood ratio as the test score, a novel f -divergence arises from the arc length of the ROC curve. By leveraging this result, we can approximate the arc length using a variational objective function with samples from two distributions. When specific parameterizations are used, this procedure leads to empirical risk minimization with two previously unknown margin-based loss functions. We also show this computational approach can be used as a non-parametric estimator to the arctangent of likelihood ratio. The effectiveness of our arc length estimator is guaranteed by our theoretical analysis: When the arctangent likelihood ratio satisfies mild smoothness conditions, this estimator achieves a rate of convergence $O_p(n^{-\beta/4})$, where β depends on the smoothness of the true arctangent likelihood ratio function.

Although the ROC curves are historically related to binary classification, this work is **not** about incorporating the ROC curve into binary classification tasks. We hope this work would inspire novel ways of using the ROC curve beyond binary classification tasks.

2 BACKGROUND

2.1 Area Under the Curve vs. Arc Length

ROC curves are frequently used to visualize binary classifiers' performance, and Area Under the Curve (AUC) has been widely used as a numerical metric for selecting a good classifier. While it is natural to assume AUC is a measure of discrepancy between positive and negative class densities (p_+ and p_-), the reality shows the opposite. Figure 1 demonstrates this phenomenon using one-dimensional densities.

p_+ is quite different from p_- in both (a) and (b), which implies the discrepancies between positive and negative distributions should be large in both cases. However, (a) has an AUC (≈ 1) that is almost twice as large as (b). p_+ and p_- are the same in (c); thus, (c)'s discrepancy should be much smaller than (a) and (b). On the contrary, (c) has a similar AUC ($\approx .5$) to (b). These two observations show the differences between distributions are not necessarily reflected by AUC.

Can we find another geometric measure that accurately quantifies the differences between class densities? Notice that other than AUC, the arc length of the ROC curve are also different among the three graphs. Both (a) and (b) have long ROC curves (≈ 2) while (c) has a shorter one ($\approx \sqrt{2}$). This observation fits our expectation earlier: the discrepancy in both (a) and (b) are large but is small in (c). It suggests that the more similar p_+ and p_- are, the shorter the ROC curve is.

Notice Figure 1 is only a toy example: In reality, ROC curves are computed on test scores rather than on the original dataset.

2.2 ROC Curve in Two Sample Setting

Suppose we have positive and negative datasets $X_+ := \{\mathbf{x}_i^+\}_{i=1}^{n_+}$ and $X_- := \{\mathbf{x}_i^-\}_{i=1}^{n_-}$ drawn from two distributions \mathbb{P}_+ and \mathbb{P}_- respectively. \mathbb{P}_+ and \mathbb{P}_- have probability density functions $p_+(\mathbf{x})$ and $p_-(\mathbf{x})$ that

are both defined on the domain $\mathcal{X} \subseteq \mathbb{R}^d$. A test score function takes a sample \mathbf{x} as input and outputs a real-valued score. Suppose we have a test score function $t(\mathbf{x}) \in \mathbb{R}$.

Let F_+ and F_- denote the Cumulative Distribution Function (CDF) of $t(\mathbf{x}^+)$ and $t(\mathbf{x}^-)$ respectively. Then False Positive Rate (FPR) is $\tilde{F}_- := 1 - F_-$ and True Positive Rate (TPR) is $\tilde{F}_+ := 1 - F_+$. If F_- is strictly increasing, **ROC curve of a score function** t is the graph of function $\tilde{F}_+[\tilde{F}_-^{-1}(s)]$, $s \in [0, 1]$. In the rest of the paper, we assume F_+ , F_- are strictly increasing.

2.3 Arc Length of ROC Curve

Due to the strict monotonicity of CDFs, \tilde{F}_+ and \tilde{F}_- form a bijective parameterization of the ROC curve in the sense that each point on this ROC curve can be written as $(\tilde{F}_-(t_0), \tilde{F}_+(t_0))$ for a unique $t_0 \in \mathbb{R}$. Using the line integral formula, the arc length of ROC curve can be expressed using derivatives of $\tilde{F}_-(t)$ and $\tilde{F}_+(t)$:

$$\begin{aligned} \widehat{\text{ROC}}(t) &:= \int_{-\infty}^{\infty} \sqrt{[\partial_t \tilde{F}_+(t)]^2 + \partial_t [\tilde{F}_-(t)]^2} dt \\ &= \int_{-\infty}^{\infty} \sqrt{p_{t_+}(t)^2 + p_{t_-}(t)^2} dt, \end{aligned} \quad (1)$$

where $p_{t_+}(t)$ is the density function of $t(\mathbf{x}^+)$ and $p_{t_-}(t)$ is the density function of $t(\mathbf{x}^-)$. Assume $p_{t_-}(t)$ is strictly positive (in which case F_- is strictly increasing), we can rewrite

$$\widehat{\text{ROC}}(t) = \int_{-\infty}^{\infty} p_{t_-}(t) \sqrt{\left[\frac{p_{t_+}(t)}{p_{t_-}(t)}\right]^2 + 1} dt. \quad (2)$$

Although (2) is an elementary result, it has been seldomly discussed in the majority body of ROC literature. (Edwards and Metz, 2007, 2008) introduced a performance metric computed over the ‘‘ROC hypersurface’’, where (2) is used to justify the usefulness of such a metric when comparing different test score functions in a classification setting.

Using (1), we can confirm a simple geometric fact:

Proposition 1. $\widehat{\text{ROC}} \in [\sqrt{2}, 2]$, regardless the choice of the test score function t .

Proof. Jensen’s inequality:

$$\widehat{\text{ROC}} = \sqrt{2} \int \sqrt{\frac{p_{t_+}^2(t)}{2} + \frac{p_{t_-}^2(t)}{2}} dt \geq \sqrt{2} \int \frac{|p_{t_+}(t)|}{2} + \frac{|p_{t_-}(t)|}{2} dt = \sqrt{2}.$$

Triangle inequality: $\widehat{\text{ROC}} \leq \int |p_{t_+}(t)| + |p_{t_-}(t)| dt = 2$. □

This result corresponds to the geometric observation that any monotone curve (such as ROC curve) starts and ends at two diagonal corners of the ROC space $[0, 1]^2$ has a length between $\sqrt{2}$ and 2.

The ratio $\frac{p_{t_+}(t)}{p_{t_-}(t)}$ can be seen as a measure of overlap between positive and negative score densities: the further the ratio deviates from 1, the less overlapped two class densities are. This explains why $\widehat{\text{ROC}}$ encodes the overlapping between densities in Figure 1.

It is natural to think, when t is appropriately chosen, $\widehat{\text{ROC}}$ also expresses the differences between positive and negative *data* densities in some way. In the next section, we show that when t is the likelihood ratio, $\widehat{\text{ROC}}(t)$ encodes the differences between $p_+(\mathbf{x})$ and $p_-(\mathbf{x})$ in the form of an f -divergence between $p_+(\mathbf{x})$ and $p_-(\mathbf{x})$.

2.4 An f -Divergence Arising from ROC curve

Notice $\widehat{\text{ROC}}(t)$ is an expectation:

$$\widehat{\text{ROC}}(t) = \mathbb{E}_{p_{t_-}(t)} \sqrt{\left[\frac{p_{t_+}(t)}{p_{t_-}(t)} \right]^2 + 1}$$

and t is a function of \mathbf{x} . Using the Law of The Unconscious Statistician, $\mathbb{E}_{g(X)}[g(X)] = \mathbb{E}_X[g(X)]$, we can express $\widehat{\text{ROC}}(t)$ in terms of an expectation with respect to the negative data density $p_-(\mathbf{x})$:

$$\widehat{\text{ROC}}(t) = \mathbb{E}_{p_-(\mathbf{x})} \sqrt{\left[\frac{p_{t_+}(\mathbf{x})}{p_{t_-}(\mathbf{x})} \right]^2 + 1}.$$

Now consider a special choice of t : $t^*(\mathbf{x}) = \frac{p_+(\mathbf{x})}{p_-(\mathbf{x})}$, a.k.a., the likelihood ratio. It can be shown that

$$\frac{p_{t_+}^*(\mathbf{x}_0)}{p_{t_-}^*(\mathbf{x}_0)} = \frac{\int_{\mathbf{x}:t^*(\mathbf{x})=\frac{p_+(\mathbf{x}_0)}{p_-(\mathbf{x}_0)}} p_+(\mathbf{x})d\mathbf{x}}{\int_{\mathbf{x}:t^*(\mathbf{x})=\frac{p_+(\mathbf{x}_0)}{p_-(\mathbf{x}_0)}} p_-(\mathbf{x})d\mathbf{x}} = \frac{p_+(\mathbf{x}_0)}{p_-(\mathbf{x}_0)} \quad (3)$$

and the second equality is due to

$$\frac{\int_D a(x)dx}{\int_D b(x)dx} = \frac{a(x)}{b(x)} = C$$

when $\frac{a(x)}{b(x)} \equiv C, \forall x \in D$. (3) is a known result (Eguchi and Copas, 2002) and is sometimes referred to as “the likelihood ratio of the likelihood ratio score is the likelihood ratio itself”. Notice that there is no obvious analogues to (3) when other score functions are used.

Finally $\widehat{\text{ROC}}(t^*)$ has an elegant form which is free from t^* :

$$\widehat{\text{ROC}}(t^*) = \mathbb{E}_{p_-(\mathbf{x})} \sqrt{\left[\frac{p_{t_+}^*(\mathbf{x})}{p_{t_-}^*(\mathbf{x})} \right]^2 + 1} = \mathbb{E}_{p_-(\mathbf{x})} \sqrt{\left[\frac{p_+(\mathbf{x})}{p_-(\mathbf{x})} \right]^2 + 1}. \quad (4)$$

To our best knowledge, (4) has not been presented in literature before.

We first show a result regarding the length of $\widehat{\text{ROC}}(t^*)$.

Proposition 2. $\widehat{\text{ROC}}(t^*)$ is the longest among all convex ROC curves.

Proof. We first show $\text{ROC}(t^*)$ is a convex curve. Define $\tilde{F}_+(\cdot; t)$ as the TPR of a test score t . To show $\text{ROC}(t^*)$ is convex, we only need to show $\tilde{F}_+(\tilde{F}_-^{-1}(s; t^*); t^*)$ is a concave function. This can be verified by checking the sign of $\partial_s^2 \tilde{F}_+(\tilde{F}_-^{-1}(s; t^*); t^*)$:

$$\begin{aligned} \partial_s \tilde{F}_+(\tilde{F}_-^{-1}(s; t^*); t^*) &= \frac{p_{t_+}^*[\tilde{F}_-^{-1}(s; t^*)]}{p_{t_-}^*[\tilde{F}_-^{-1}(s; t^*)]} = \tilde{F}_-^{-1}(s; t^*), \\ \partial_s^2 \tilde{F}_+(\tilde{F}_-^{-1}(s; t^*); t^*) &= -\frac{1}{p_{t_-}^*(\tilde{F}_-^{-1}(s; t^*))} < 0. \end{aligned}$$

Moreover, at any FPR level $s \in [0, 1]$, Neyman-Pearson Lemma implies

$$\tilde{F}_+(\tilde{F}_-^{-1}(s; t^*); t^*) \geq \tilde{F}_+(\tilde{F}_-^{-1}(s; t); t), \forall t.$$

In words, $\text{ROC}(t^*)$ dominates all other ROC curves. Since $\text{ROC}(t^*)$ is convex and encloses all other ROC curves, our claim follows Archimedes’s Second Axiom: among all convex curves with the same endpoints, the one encloses all other curves has the longest arc length. \square

Below we show a key result in our paper: A novel f -divergence arises from the arc length of the optimal ROC curve. This shows that the arc length of the optimal ROC can indeed be used as a difference measure between two distributions.

Proposition 3 (ROC divergence). $\widehat{\text{ROC}}(t^*) - \sqrt{2}$ is an f -divergence between $p_+(\mathbf{x})$ and $p_-(\mathbf{x})$.

Proof. By definition,

$$\widehat{\text{ROC}}(t^*) - \sqrt{2} = \int_{\mathcal{X}} p_-(\mathbf{x}) f \left[\frac{p_+(\mathbf{x})}{p_-(\mathbf{x})} \right] d\mathbf{x},$$

where $f(z) = \sqrt{z^2 + 1} - \sqrt{2}$, is convex and equals zero if and only if $z = 1$. \square

By definition, ROC divergence is symmetric. Moreover, as a result of Proposition 1, ROC divergence is upper bounded by $2 - \sqrt{2}$ and lower bounded by 0. Now we generalize our statements above to a family of *rescaled* ROC curves. Every curve in this family corresponds to an f -divergence.

Definition 1. A *rescaled ROC curve*, denoted as $\text{ROC}(t^*; a, b)$, is the graph of the function

$$a\tilde{F}_+(\tilde{F}_-^{-1}(\frac{1}{b} \cdot s)), s \in [0, b],$$

where $a, b \neq 0$. **ROC divergence family** is defined as

$$D_{a,b}[p_+|p_-] := \widehat{\text{ROC}}(t^*; a, b) - \sqrt{\left(\frac{a}{b}\right)^2 + 1},$$

where $a, b \neq 0$.

Proposition 4. Given $a, b \neq 0$, we have

$$\widehat{\text{ROC}}(t^*; a, b) = \int_{\mathcal{X}} bp_-(\mathbf{x}) \sqrt{\left[\frac{ap_+(\mathbf{x})}{bp_-(\mathbf{x})}\right]^2 + 1} d\mathbf{x}.$$

Moreover, $D_{a,b}[p_+|p_-] = \int_{\mathcal{X}} bp_-(\mathbf{x}) f_{a,b} \left[\frac{ap_+(\mathbf{x})}{bp_-(\mathbf{x})} \right] d\mathbf{x}$, where $f_{a,b}(z) = \sqrt{z^2 \cdot \frac{a^2}{b^2} + 1} - \sqrt{\left(\frac{a}{b}\right)^2 + 1}$.

Notice the rescaled curve $\text{ROC}(t^*; a, b)$ has a parameterization $(b\tilde{F}_-(t^*), a\tilde{F}_+(t^*))$. Then the proof of the above statement follows the same argument presented for the unscaled ROC curve in Section 2.3 and 2.4. This family of rescaled ROC curves becomes useful in later sections.

3 Estimating Arc Length of $\text{ROC}(t^*)$

3.1 A Variational Objective

It is natural to consider approximating $\widehat{\text{ROC}}(t^*)$ numerically using samples: In tasks (such as GAN) where $\widehat{\text{ROC}}(t^*)$ would be a good performance metric, we normally do not have access to p_+ or p_- but samples from two distributions. Thus we must be able to compute the arc length using samples only. Now we leverage that $\widehat{\text{ROC}}(t^*) - \sqrt{2}$ is an f -divergence to construct an estimator of $\widehat{\text{ROC}}(t^*)$ using samples from X_- and X_+ only. Utilizing Fenchel's duality (Hiriart-Urruty and Lemaréchal, 2004), Nguyen et al. shows that an f -divergence has a variational representation:

$$\begin{aligned} D_f(p_+|p_-) &= \int_{\mathcal{X}} p_-(\mathbf{x}) f \left[\frac{p_+(\mathbf{x})}{p_-(\mathbf{x})} \right] d\mathbf{x} = \int_{\mathcal{X}} p_-(\mathbf{x}) \sup_u \left\{ u(\mathbf{x}) \cdot \left[\frac{p_+(\mathbf{x})}{p_-(\mathbf{x})} \right] - f'[u(\mathbf{x})] \right\} d\mathbf{x} \\ &= \sup_u \int_{\mathcal{X}} p_+(\mathbf{x}) u(\mathbf{x}) - \int_{\mathcal{X}} p_-(\mathbf{x}) f'[u(\mathbf{x})] d\mathbf{x}, \end{aligned}$$

where f' is the convex conjugate of f and the supremum is taken over all measurable functions. In the case of ROC divergence, $f(z) = \sqrt{z^2 + 1} - \sqrt{2}$, $z \in [0, \infty]$ ¹ has a convex conjugate $f'(z') = -\sqrt{1 - z'^2} - \sqrt{2}$, $z' \in [0, 1]$. Rewriting $\widehat{\text{ROC}}(t^*) - \sqrt{2}$ using the above variational representation and drop the $-\sqrt{2}$ for simplicity, we obtain:

$$\widehat{\text{ROC}}(t^*) = \sup_{u \in [0, 1]} \mathbb{E}_{p_+}[u(\mathbf{x})] + \mathbb{E}_{p_-}[\sqrt{1 - u^2(\mathbf{x})}].$$

Noting the constraint $u \in [0, 1]$, we reparameterize $u(\mathbf{x}) = \sin[v(\mathbf{x})]$, where $v \in [0, \pi/2]$:

$$\widehat{\text{ROC}}(t^*) = \sup_{v \in [0, \pi/2]} \mathbb{E}_{p_+} \sin[v(\mathbf{x})] + \mathbb{E}_{p_-} \cos[v(\mathbf{x})]. \quad (5)$$

Differentiating (5) for v , we can see the supremum is attained at $v^*(\mathbf{x}) = \arctan \left[\frac{p_+(\mathbf{x})}{p_-(\mathbf{x})} \right]$. In other words, the optimal choice of v is the arctangent density ratio function. When optimizing (5) in practice, we need to restrict v within some function class, and v^* will serve as the guiding principle when designing such a class, as we will discuss later.

As we have already seen in the proof of Proposition 2, the tangent of $\widehat{\text{ROC}}(t^*)$ at an FPR level $s_0 \in [0, 1]$ is

$$\partial_s \tilde{F}_+(\tilde{F}_-^{-1}(s_0)) = \tilde{F}_-^{-1}(s_0) = \frac{p_{t_+}^*(\tilde{F}_-^{-1}(s_0))}{p_{t_-}^*(\tilde{F}_-^{-1}(s_0))} = \frac{p_+(\mathbf{x}_0)}{p_-(\mathbf{x}_0)},$$

where \mathbf{x}_0 is any point in \mathcal{X} that satisfies the equality $\frac{p_+(\mathbf{x}_0)}{p_-(\mathbf{x}_0)} = \tilde{F}_-^{-1}(s_0)$. It means, $v^*(\mathbf{x})$ is the *slope angle* of $\widehat{\text{ROC}}(t^*)$. The boundary constraint for $v(\mathbf{x})$ in (5) coincides with the geometric fact that the slope angle of any ROC curve is in between 0 and $\pi/2$.

Let us consider estimating $\widehat{\text{ROC}}(t^*; a, b)$. From Proposition 4, we see that $f_{a,b}(z) = f(\frac{a}{b} \cdot z) + C$, where C is a constant, so the convex conjugate $f'_{a,b}(z') = f'(\frac{b}{a}z') + C$. Using the same variational trick,

$$b\mathbb{E}_{p_-} \left[f_{a,b} \left(\frac{ap_+(\mathbf{x})}{bp_-(\mathbf{x})} \right) \right] = \sup_u b\mathbb{E}_{p_-} \left[\frac{a}{b}u(\mathbf{x}) - f' \left(\frac{ap_+(\mathbf{x})}{bp_-(\mathbf{x})} \right) \right]$$

Drop the constant and apply the reparameterization $u(\mathbf{x}) = \sin[v(\mathbf{x})]$:

$$\widehat{\text{ROC}}(t^*; a, b) = \sup_{v \in [0, \pi/2]} \int ap_+(\mathbf{x}) \sin[v(\mathbf{x})] + \int bp_-(\mathbf{x}) \cos[v(\mathbf{x})] d\mathbf{x} \quad (6)$$

and the supremum is attained at $v^*(\mathbf{x}) = \arctan \left[\frac{ap_+(\mathbf{x})}{bp_-(\mathbf{x})} \right]$. This result plays an important role in the following section.

Using (5), we can obtain a relationship between $\widehat{\text{ROC}}(t^*)$ and the total variation distance between \mathbb{P}_+ and \mathbb{P}_- (denoted as $\text{TV}(\mathbb{P}_+, \mathbb{P}_-)$):

Proposition 5.

$$\text{TV}(\mathbb{P}_+, \mathbb{P}_-) + 1 \leq \widehat{\text{ROC}}(t^*) \leq \frac{\pi}{2} \text{TV}(\mathbb{P}_+, \mathbb{P}_-) + \frac{\pi}{2}.$$

Proof can be found at Section A. This proposition states that the arc length of the optimal ROC curve has a lower and upper bound expressed via $\text{TV}(\mathbb{P}_+, \mathbb{P}_-)$, which further justifies $\widehat{\text{ROC}}(t^*)$ as a measure of discrepancies between \mathbb{P}_+ and \mathbb{P}_- .

¹ p_+/p_- cannot be negative.

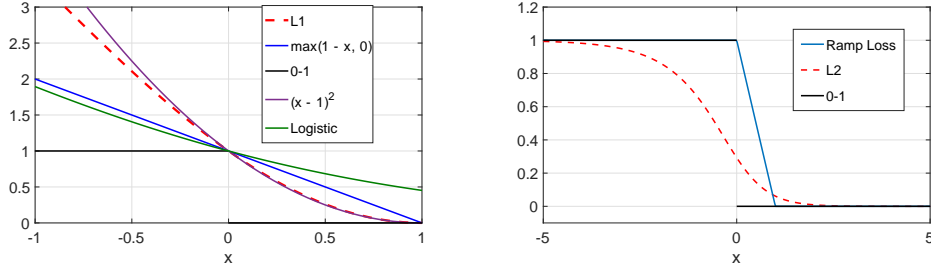


Figure 2: Zoo of loss functions: \mathcal{L}_1 is shown in the upper plot with other convex surrogate loss functions. \mathcal{L}_2 is shown in the plot below with Ramp and 0-1 loss. Note that despite the similarity between \mathcal{L}_1 and the squared loss, \mathcal{L}_1 is *undefined* outside of $[-1, 1]$.

3.2 From Arc Length to Binary Classification Losses

From now on, we will constantly encounter summations over different datasets. To reduce visual clutter, we introduce the following rule: $\sum_i^{n+} f(\mathbf{x}_i)$ should be understood as $\sum_i^{n+} f(\mathbf{x}_i^+)$ and $\sum_i^{n++n-} f(\mathbf{x}_i)$ should be understood as $\sum_i^{n+} f(\mathbf{x}_i^+) + \sum_i^{n-} f(\mathbf{x}_i^-)$: The *superscript* of the summation symbol indicates over what dataset(s) the sum is taken.

It is tempting to use (5) as a binary classifier: The optimal $v^* = \arctan \left[\frac{p_+(\mathbf{x})}{p_-(\mathbf{x})} \right]$ is a natural candidate for predicting function. Indeed, it is known that if an f -divergence satisfies some regularity conditions, there exist convex surrogate loss functions that induce the corresponding f -divergence (see Theorem 1, (Nguyen et al., 2009) for details). In this section, we show two novel loss functions arise from (5). For now, we assume $n_+ = n_- = n_0$, but this restriction will be lifted later.

Parametrizing $\arctan \left[\frac{p_+(\mathbf{x})}{p_-(\mathbf{x})} \right]$ **directly** We can simply restrict v in a (parametric/non-parametric) function class \mathcal{F} and solve the sample version of (5). Consider the following optimization:

$$\max_{v \in [0, \pi/2], v \in \mathcal{F}} \frac{1}{n_+} \sum_{i=1}^{n_+} \sin(v(\mathbf{x}_i)) + \frac{1}{n_-} \sum_{i=1}^{n_-} \cos(v(\mathbf{x}_i)), \quad (7)$$

Letting $v' = (v - \pi/4)/(\pi/4) \in [-1, 1]$ and adopting the classical classification notation: $\{(y_i, \mathbf{x}_i)\}_{i=1}^{n_++n_-}$, $y_i \in \{-, +\}$, (7) can be recast into an empirical loss minimization problem:

$$\min_{v' \in [-1, 1]} \sum_{y \in \{-, +\}} \frac{1}{n_0} \sum_{i=1}^{n_y} \mathcal{L}_1(y, v'(\mathbf{x}_i)), \quad (8)$$

where the loss function

$$\mathcal{L}_1(y, z) := \frac{\{-\sin[\frac{\pi}{4} + \frac{\pi}{4} \cdot y \cdot z] + 1\}}{-\sin(\frac{\pi}{4}) + 1}$$

used in (8) is a convex surrogate to 0-1 loss, defined on $\{-1, 1\} \times [-1, 1]$. See Figure 2 for a plot of \mathcal{L}_1 and other common classification loss functions.

Parametrizing $\log \left[\frac{p_+(\mathbf{x})}{p_-(\mathbf{x})} \right]$ Since v^* is the arctangent of the likelihood ratio, we can leverage this information and introduce some mild assumptions on p_+ and p_- . When $p_+(\mathbf{x})$ and $p_-(\mathbf{x})$ are both members of the exponential family and share the same sufficient statistic $\mathbf{h}(\mathbf{x})$, then $\exists \mathbf{v}_0 \in \mathbb{R}^m$, $\log \left[\frac{p_+(\mathbf{x})}{p_-(\mathbf{x})} \right] = \langle \mathbf{v}_0, \mathbf{h}(\mathbf{x}) \rangle + C$,

where C is a constant. If we choose to parameterize the log likelihood ratio using a linear model $\langle \mathbf{v}, \mathbf{h}(\mathbf{x}) \rangle + v_0$, (7) becomes

$$\max_{\mathbf{v} \in \mathbb{R}^m, v_0 \in \mathbb{R}} \frac{1}{n_+} \sum_{i=1}^{n_+} \sin[\arctan(\exp(\langle \mathbf{v}, \mathbf{h}(\mathbf{x}_i) \rangle + v_0))] + \frac{1}{n_-} \sum_{i=1}^{n_-} \cos[\arctan(\exp(\langle \mathbf{v}, \mathbf{h}(\mathbf{x}_i) \rangle + v_0))]. \quad (9)$$

We do not have to restrict the optimization to a bounded domain as $\log \left[\frac{p_+(\mathbf{x})}{p_-(\mathbf{x})} \right] \in \mathbb{R}$. Similarly, we can recast (9) into an empirical loss minimization problem using classic binary classification notations:

$$\min_{\mathbf{v} \in \mathbb{R}^m} \sum_{y \in \{-, +\}} \frac{1}{n_0} \sum_{i=1}^{n_y} \mathcal{L}_2(y, \langle \mathbf{v}, \mathbf{h}(\mathbf{x}_i) \rangle), \quad (10)$$

The loss function

$$\mathcal{L}_2(y, z) := -\sin\{\arctan[\exp(y \cdot z)]\} + 1,$$

defined on $\{-, +\} \times \mathbb{R}$ is non-convex and is similar to *Ramp Loss*. See Figure 2 for a visualization. Comparing to Ramp Loss, this loss is more merciful on marginally incorrectly-classified points. \mathcal{L}_2 can be seen as a probabilistic version of Ramp Loss, just as logistic regression is a probabilistic version of Hinge Loss.

Since \mathcal{L}_1 and \mathcal{L}_2 are both *margin-based losses* ($\mathcal{L}(y, z) = \mathcal{L}(y \cdot z)$), they are drop-in replacements for other margin-based loss functions (such as Hinge loss, Ramp Loss, or Logistic Loss).

Now we generalize the above results to unbalanced cases (i.e., $n_+ \neq n_-$). Consider the empirical version of (6) with $a = n_+$ and $b = n_-$.

$$\widehat{\text{ROC}}(t^*; n_+, n_-) \approx \max_{v \in [0, \pi/2]} \frac{1}{n_+} \sum_{i=1}^{n_+} n_+ \sin[v(\mathbf{x}_i)] + \frac{1}{n_-} \sum_{i=1}^{n_-} n_- \cos[v(\mathbf{x}_i)].$$

Similarly, by either parameterizing $\arctan \left[\frac{n_+ p_+(\mathbf{x})}{n_- p_-(\mathbf{x})} \right]$ or $\log \left[\frac{n_+ p_+(\mathbf{x})}{n_- p_-(\mathbf{x})} \right]$, we can convert the above optimization into an empirical loss minimization problem:

$$\min_{v \in [0, \pi/2]} \sum_{y \in \{-, +\}} \frac{1}{n_y} \cdot n_y \sum_{i=1}^{n_y} \mathcal{L}(y_i, v(\mathbf{x}_i))$$

where \mathcal{L} depends on the parameterization.

In conclusion, approximating $\widehat{\text{ROC}}(t^*; n_+, n_-)$ leads to empirical loss minimization problems with two novel loss functions. They are drop-in replacements for other margin-based loss functions. It is also natural to consider these loss functions in multi-class classification problems by employing one-versus-the other or one-versus-one rules. We suspect this approach would lead to the approximation of a more general type of ROC curve (Ferri et al., 2003) and the justification of this will be future work.

4 ESTIMATING ARCTANGENT of DENSITY RATIO

4.1 Theoretical Analysis

Now we derive the theoretical guarantee of the sample objective functions in Section 3.2: Since these objective functions are derived by parameterizing either log or arctan density ratio function, they are naturally estimators to $\arctan \frac{p_+(\mathbf{x})}{p_-(\mathbf{x})}$ and $\log \frac{p_+(\mathbf{x})}{p_-(\mathbf{x})}$. In this paper, we focus on (7), since (9) is non-convex and presents some extra challenges for the theoretical analysis. Note that due to the Lipschitz continuity of (7), the effectiveness of the arctangent ratio estimator can be directly translated into the effectiveness of estimating the $\widehat{\text{ROC}}(t^*)$.

Let us consider the following optimization.

$$\begin{aligned} \hat{f} &:= \operatorname{argmin}_{f \in \mathcal{H}} \ell(f) + \frac{\lambda}{2} \|f\|_{\mathcal{H}}^2, \quad \ell(f) := -\frac{1}{n_+} \sum_{i=1}^{n_+} \sin \langle f, \varphi(\mathbf{x}_i) \rangle - \frac{1}{n_-} \sum_{i=1}^{n_-} \cos \langle f, \varphi(\mathbf{x}_i) \rangle \\ \text{s.t: } &\langle f, \varphi(\mathbf{x}) \rangle \in [0, \frac{\pi}{2}], \quad \forall \mathbf{x} \in X_+ \cup X_-, \end{aligned} \quad (11)$$

where \mathcal{H} is a Reproducing Kernel Hilbert Space (RKHS) (Scholkopf and Smola, 2001) with a positive definite kernel $k(\mathbf{x}, \mathbf{x}') = \langle \varphi(\mathbf{x}), \varphi(\mathbf{x}') \rangle$. (11) is a relaxation of (7): The boundedness constraint for v is only enforced at sample points in our datasets rather than over the entire domain as shown in (7). Moreover, RKHS \mathcal{H} replaces the function class \mathcal{F} . (11) is a strictly convex optimization, hence it must have a unique solution \hat{f} if it exists.

Now we show that $\langle \hat{f}, \varphi(\mathbf{x}) \rangle$ converges to the true arctangent density ratio (or its projection in \mathcal{H}) as the number of samples goes to infinity. First we list a few regularity conditions.

Assumption 1. *There exists a unique $f^* \in \mathcal{H}$, such that $\mathbb{E}[\nabla_f \ell(f^*)] = 0$ and $\langle f^*, \varphi(\mathbf{x}) \rangle \in [0, \pi/2]$ holds for all $\mathbf{x} \in \mathcal{X}$.*

Proposition 6. *If there exists a unique f^* , such that $\langle f^*, \varphi(\mathbf{x}) \rangle = \arctan \left[\frac{p_+(\mathbf{x})}{p_-(\mathbf{x})} \right]$, Assumption 1 holds.*

Proof can be found in Section C. Proposition 6 states, as long as our model is correctly specified and identifiable, Assumption 1 holds. Note Assumption 1 also covers *some* misspecified models: It is possible that an $f^* \in \mathcal{H}$ that satisfies $\mathbb{E}[\nabla_f \ell(f^*)] = 0$ does not meet the boundedness constraint $[0, \pi/2]$. To estimate such f^* , we can consider an expanded constraint $[0 - \epsilon, \pi/2 + \epsilon]$, $\epsilon > 0$ for (11), but this expansion also makes (11) non-convex and its theoretical analysis using the current proof is cumbersome. Thus, in this paper, we only consider situations where Assumption 1 holds: This includes situations where the model is correctly specified and some situations where the model is misspecified.

Assumption 2. *Let n_{\min} denote $\min(n_+, n_-)$. There exists a subspace $\mathcal{H}^* := \{f \in \mathcal{H} \mid \|f - f^*\|_{\mathcal{H}}^2 \leq \delta_{n_{\min}}^2\}$, such that $\forall f \in \mathcal{H}^*, \forall \mathbf{x} \in X_+ \cup X_-, \langle f, \varphi(\mathbf{x}) \rangle \in (0, \frac{\pi}{2})$ holds with high probability. The sequence $\delta_{n_{\min}}$ is monotonically decreasing as n_{\min} grows to infinity.*

Assumption 2 states all f from a vicinity of f^* is in the interior of (11)'s feasible region with high probability. The following proposition gives a sufficient condition under which Assumption 2 holds.

Proposition 7. *Suppose $\|\varphi(\mathbf{x})\|_{\mathcal{H}} \leq 1$. If our model is correctly specified as described in Proposition 6 and $\arctan \left[\frac{p_+(\mathbf{x})}{p_-(\mathbf{x})} \right] \in [R_1, R_2]$, $\forall \mathbf{x} \in \mathcal{X}$, for some R_1 and R_2 such that $\pi/2 > R_2 > R_1 > 0$, then there exists $N > 0$ such that Assumption 2 holds when $n_{\min} > N$.*

Proof. $\forall f \in \mathcal{H}^*, |\langle f, \varphi(\mathbf{x}) \rangle - \langle f^*, \varphi(\mathbf{x}) \rangle| \leq \|f - f^*\|_{\mathcal{H}} \|\varphi(\mathbf{x})\|_{\mathcal{H}} \leq \delta_{n_{\min}}$ due to Lipschitz continuity. If $\delta_{n_{\min}} < \min(R_1, \frac{\pi}{2} - R_2)$ then $\langle f, \varphi(\mathbf{x}) \rangle \in (0, \frac{\pi}{2})$ holds uniformly for every $\mathbf{x} \in \mathcal{X}$. As $\delta_{n_{\min}}$ is a decaying sequence, there always exists an N such that $\delta_{n_{\min}} \leq \min(R_1, \frac{\pi}{2} - R_2)$ holds for $n_{\min} \geq N$. \square

Since we use RKHS as the estimator function class, our final assumption is that f^* should be reasonably smooth. While in previous works, such type of assumption depends on the decay of integral operator's eigenvalues (Steinwart et al., 2009; Fukumizu, 2009). In this paper, we measure the smoothness using the *range space* technique. This is a method that has recently been adopted in (Fukumizu et al., 2013; Sriperumbudur et al., 2017). Let:

$$\Sigma_f := \mathbb{E}[\nabla_f^2 \ell(f)] = \mathbb{E}_+[\sin \langle f, \varphi(\mathbf{x}) \rangle \cdot \varphi(\mathbf{x}, \cdot) \otimes \varphi(\mathbf{x}, \cdot)] + \mathbb{E}_-[\cos \langle f, \varphi(\mathbf{x}) \rangle \cdot \varphi(\mathbf{x}, \cdot) \otimes \varphi(\mathbf{x}, \cdot)],$$

where \otimes denotes outer product. Given $f_0 \in \mathcal{H}$, Σ_{f_0} is an integral operator on $u \in \mathcal{H}$,

$$\Sigma_{f_0} u = \mathbb{E}_+[\sin \langle f_0, \varphi(\mathbf{x}) \rangle \cdot \varphi(\mathbf{x}, \cdot) \cdot u(\mathbf{x})] + \mathbb{E}_-[\cos \langle f_0, \varphi(\mathbf{x}) \rangle \cdot \varphi(\mathbf{x}, \cdot) \cdot u(\mathbf{x})].$$

By definition Σ_{f_0} is a positive, self-adjoint operator, in the sense that $\langle u, \Sigma_{f_0} u \rangle \geq 0$, $\langle u, \Sigma_{f_0} v \rangle = \langle \Sigma_{f_0} u, v \rangle$, $\forall v, u \in \mathcal{H}$. Moreover, some algebra shows that Σ_{f_0} is also a bounded and compact operator. See Section E for more details.

We assume the true arctangent ratio function (or its projection) is in the range space of Σ_{f^*} .

Assumption 3. Let $\mathcal{R}(\Sigma_{f^*})$ denote the range space of Σ_{f^*} . There exists $0 < \beta \leq 1$, $f^* \in \mathcal{R}(\Sigma_{f^*}^\beta)$, where C^β is the fraction power of a compact, positive and self-adjoint operator C .

Note that the larger β is, the smoother the functions in the range space are. More discussions on the range space assumption can be found in Section 4.2, (Sriperumbudur et al., 2017). Now we are ready to state our theorem:

Theorem 1 (Convergence Rate of \hat{f}). Suppose Assumption 1, 2 and 3 hold and \hat{f} exists. If $\|\varphi(\mathbf{x})\|_{\mathcal{H}} \leq 1$ and

$$\lambda = \frac{T}{n_{\min}^{1/4}}, \quad \frac{K}{n_{\min}^{\beta/4}} \leq \delta_{n_{\min}} \leq \frac{4}{\max(B_+, B_-)},$$

where

$$B_+ = \|(\Sigma_{f^*} + \lambda \mathbf{I})^{-1} \mathbb{E}_+[\varphi(\mathbf{x})]\|_{\mathcal{H}},$$

$$B_- = \|(\Sigma_{f^*} + \lambda \mathbf{I})^{-1} \mathbb{E}_-[\varphi(\mathbf{x})]\|_{\mathcal{H}},$$

and $T \geq 1, K > 0$ are constants that do not depend on n_{\min} , then there exists a constant $N > 0$ such that when $n_{\min} > N$,

$$\|\hat{f} - f^*\|_{\mathcal{H}} = O_p(n_{\min}^{-\beta/4}).$$

The proof can be found at Section B.

Theorem 1 shows that \hat{f} is indeed a good estimator for $\arctan \left[\frac{p_+(\mathbf{x})}{p_-(\mathbf{x})} \right]$ under some mild conditions. In fact, Theorem 1 holds without not explicitly requiring the density ratio $\frac{p_+(\mathbf{x})}{p_-(\mathbf{x})}$ to be lower and upper bounded, a condition that is required for some parametric density ratio estimation (Kim et al., 2021). As we previous mentioned, the arctangent density ratio is the slope angle of the ROC curve. The slope angle of ROC has been widely used to select threshold for binary classifiers. It will be an interesting future work to connect our estimator with such applications. Estimating arctangent density ratio itself may have important practical applications such as outlier detection (Hido et al., 2011) and GAN (Goodfellow et al., 2014).

4.2 Dual Objective

One can solve (11) directly if \mathcal{H} is a finite dimensional RKHS. To handle an infinite dimensional RKHS (such as the one induced by Gaussian kernel), we need the Lagrangian dual form of (11):

$$\max_{\substack{\mathbf{t} \in [0,1]^{n_+}, \mathbf{t}' \in [0,1]^{n_-}, \\ \boldsymbol{\xi} \geq 0, \boldsymbol{\xi}' \geq 0, \boldsymbol{\alpha}}} - \frac{1}{n_+} \sum_{i=1}^{n_+} \eta(t_i) - \frac{1}{n_-} \sum_{i=1}^{n_-} \eta(t'_i) + \frac{1}{n_+} \sum_{i=1}^{n_+} t_i \arccos(t_i) - \frac{1}{n_-} \sum_{i=1}^{n_-} t'_i \arcsin(t'_i) - \frac{\pi}{2} \sum_{i=1}^{n_++n_-} \xi_i - \frac{\boldsymbol{\alpha}^\top \mathbf{K} \boldsymbol{\alpha}}{4\lambda},$$

$$\text{subject to: } t_i = n_+(-\xi_{i+} + \xi'_{i+} + \alpha_{i+}), t'_i = n_-(\xi_{i-} - \xi'_{i-} - \alpha_{i-}), \sum_{i=1}^{n_++n_-} \alpha_i = 0. \quad (12)$$

where $\eta(t) = \sqrt{1-t^2}$, \mathbf{K} is the kernel matrix and $\boldsymbol{\xi}, \boldsymbol{\xi}', \boldsymbol{\alpha} \in \mathbb{R}^{n_++n_-}$. Here $i+$ is the index for positive samples, as in, \mathbf{x}_{1+} is the first positive sample. The arctangent density ratio estimator is given by:

$$\hat{f}(\mathbf{x}) := \frac{1}{2\lambda} \sum_{i=1}^{n_++n_-} \hat{\alpha}_i k(\mathbf{x}_i, \mathbf{x}) - \frac{1}{2\lambda} \sum_{i=1}^{n_+} \hat{\alpha}_i k(\mathbf{x}_i, \mathbf{x}_{i_0}^+) + \arccos(\hat{t}_{i_0}),$$

where i_0 is the index of any sample in the positive dataset. Derivations can be found in Section D.

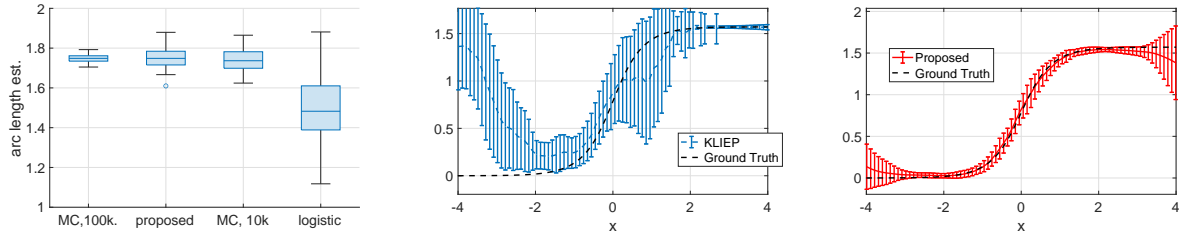


Figure 3: L: $\widehat{\text{ROC}}(t^*)$ arc length estimation. M, R: Estimation of the arctangent density ratio function.

4.3 Numerical Experiments

We draw 50 samples from $\mathcal{N}(1, 1)$ and $\mathcal{N}(-1, 1)$ as X_+ and X_- and estimate $\widehat{\text{ROC}}(t^*)$ using three different approaches:

- Compute $\frac{p_+(\mathbf{x})}{p_-(\mathbf{x})}$ using the ground truth and approximate $\widehat{\text{ROC}}(t^*)$ using Monte Carlo (MC).
- Optimize (11) (by solving (12)) and use the optimal objective value as the estimate of $\widehat{\text{ROC}}(t^*)$.
- Run logistic regression, then use the estimated density ratio function (Gutmann and Hirayama, 2012) together with samples in X_- to approximate $\widehat{\text{ROC}}(t^*)$ according to (4).

The approximation results (over 72 runs) are shown in Figure 3. It can be seen that the proposed approach, using 100 samples in total achieved approximately the same level of accuracy as the MC approach using 10k samples and the ground truth information. Logistic regression on the other hand, does not give an accurate estimation of $\widehat{\text{ROC}}(t^*)$.

Then we draw 100 samples as X_+ and X_- and compare the estimated arctangent density ratio with the another density ratio estimator KLIEP (Sugiyama et al., 2012). The estimated arctangent density ratio with standard deviation (over 72 runs) are plotted in Figure 3. Result shows, our estimated arctangent ratio is closer to the ground truth and has a much smaller standard deviation.

All methods use Gaussian kernel, hyperparameters are tuned using cross validation. See Section F for details of parameter tuning².

5 Conclusion

In this paper, we showed that an f -divergence arises from the arc length of the ROC curve. This result provides justification of using the ROC curve for two-sample applications, including change-detection, two-sample tests and GAN. Moreover, we show that the arc length can be approximated using samples from two distributions, which can be convenient for applications that only have access to samples. We also show that the arc length has lower and upper bounds which can be expressed via total variational distances. Finally, we study the convergence of the arc length estimator which is also an estimator of the arctangent likelihood ratio function. We show it has a non-parametric convergence rate of $O(n^{-\beta/4})$, $\beta \in [0, 1]$.

Acknowledgements

The author thanks Prof. Peter Flach and Dr. Hao Song for helpful discussions.

²Code will be released soon!

Note: We use $\mathbb{E}_+[f(\mathbf{x})]$ to denote $\int p_+(\mathbf{x})f(\mathbf{x})d\mathbf{x}$ from now on.

A Proof of Proposition 5

Proof. Using the integral probability metric representation of $\text{TV}(\mathbb{P}_+, \mathbb{P}_-)$ (Sriperumbudur et al., 2012), we can write:

$$\begin{aligned} \frac{\pi}{2}\text{TV}(\mathbb{P}_+, \mathbb{P}_-) &= \sup_{\|v\|_\infty \leq 1} \mathbb{E}_{p_+} \left[\frac{\pi}{2} \cdot \frac{(v(\mathbf{x}) + 1)}{2} \right] - \mathbb{E}_{p_-} \left[\frac{\pi}{2} \cdot \frac{(v(\mathbf{x}) + 1)}{2} \right] \\ &= \sup_{v' \in [0, \pi/2]} \mathbb{E}_{p_+} v'(\mathbf{x}) + \mathbb{E}_{p_-} [-v'(\mathbf{x})] \\ &\geq \sup_{v' \in [0, \pi/2]} \mathbb{E}_{p_+} \sin[v'(\mathbf{x})] + \mathbb{E}_{p_-} \cos[v'(\mathbf{x})] - \frac{\pi}{2} \\ &= \widehat{\text{ROC}}(t^*) - \frac{\pi}{2}. \end{aligned}$$

Similarly, multiplying both sides of the second equality above by $\frac{2}{\pi}$, we obtain

$$\begin{aligned} \text{TV}(\mathbb{P}_+, \mathbb{P}_-) &= \sup_{v' \in [0, \pi/2]} \mathbb{E}_{p_+} \frac{2}{\pi} v'(\mathbf{x}) + \mathbb{E}_{p_-} \left[-\frac{2}{\pi} v'(\mathbf{x}) \right] \\ &\leq \sup_{v' \in [0, \pi/2]} \mathbb{E}_{p_+} \sin(v'(\mathbf{x})) + \mathbb{E}_{p_-} [\cos v'(\mathbf{x}) - 1] \\ &= \widehat{\text{ROC}}(t^*) - 1 \end{aligned}$$

□

B Proof of Theorem 1

To reduce visual clutter, in this section, $\|f\|$ represents the Hilbert space norm of f , defined as $\sqrt{\langle f, f \rangle}$.

Proof. Define $\mathcal{H}^* := \{f \in \mathcal{H} \mid \|f - f^*\|^2 \leq \delta^2\}$. Consider an optimization that is similar to (11):

$$\tilde{f} := \underset{f \in \mathcal{H}^*}{\text{argmin}} \ell(f) + \frac{\lambda}{2} \|f\|^2 \quad (13)$$

Define $\tilde{u} := \tilde{f} - f^*$ and we have the following equality due to the KKT conditions of (13)

$$\nabla_f \ell(\tilde{f}) + \lambda \tilde{f} + 2\nu \tilde{u} = 0.$$

Multiplying both sides by $\tilde{s} = (\Sigma_{f^*} + \lambda \mathbf{I})^{-1} \tilde{u}$, we have

$$\langle \tilde{s}, \nabla_f \ell(\tilde{f}) + \lambda \tilde{f} + 2\nu \tilde{u} \rangle = 0.$$

Let $g(f) := \langle \tilde{s}, \nabla_f \ell(f) + \lambda f + 2\nu(f - f^*) \rangle$, we can applying Mean Value Theorem (MVT) on the scalar valued function $g(f)$:

$$g(\tilde{f}) - g(f^*) = \nabla_f g(\bar{f}) \tilde{u}, \quad (14)$$

where $\bar{f} = af^* + (1-a)\tilde{f}$ for some $a \in [0, 1]$. Knowing $g(\tilde{f}) = 0$ and $g(f^*) = \langle \tilde{s}, \nabla_f \ell(f^*) + \lambda f^* \rangle$, we can translate (14) into

$$\langle \tilde{s}, -\nabla_f \ell(f^*) - \lambda f^* \rangle = \langle \tilde{s}, [\nabla_f^2 \ell(\bar{f}) + \lambda \mathbf{I} + 2\nu \mathbf{I}] \tilde{u} \rangle, \quad (15)$$

where \mathbf{I} is the identify matrix. Focusing on the RHS, we have

$$\begin{aligned}
\langle \tilde{s}, [\nabla_f^2 \ell(\bar{f}) + \lambda \mathbf{I} + 2\nu \mathbf{I}] \tilde{u} \rangle &\geq \langle \tilde{s}, [\nabla_f^2 \ell(\bar{f}) + \lambda \mathbf{I}] \tilde{u} \rangle \\
&\geq \underbrace{\langle (\boldsymbol{\Sigma}_{f^*} + \lambda \mathbf{I})^{-1} \tilde{u}, [\boldsymbol{\Sigma}_{f^*} + \lambda \mathbf{I}] \tilde{u} \rangle}_{\|\tilde{u}\|^2} - \underbrace{\langle \tilde{s}, [\boldsymbol{\Sigma}_{f^*} - \boldsymbol{\Sigma}_{\bar{f}}] \tilde{u} \rangle}_a - \underbrace{\langle \tilde{s}, [\boldsymbol{\Sigma}_{\bar{f}} - \nabla_f^2 \ell(\bar{f})] \tilde{u} \rangle}_b \\
&\geq \|\tilde{u}\|^2 - a - b.
\end{aligned} \tag{16}$$

The second line is due to the fact that $\langle 2\nu \tilde{s}, \tilde{u} \rangle \geq 0$. Use the inequality (16) on (15), we get the inequality

$$\langle \tilde{s}, -\nabla_f \ell(f^*) - \lambda f^* \rangle \geq \|\tilde{u}\|^2 - a - b. \tag{17}$$

First, let us inspect a . Using MVT on $\sin \langle f, \varphi(\mathbf{x}) \rangle$, $f \in \mathcal{H}^*$ and apply Hölder's inequality, we get

$$\sin \langle f^*, \varphi(\mathbf{x}) \rangle - \sin \langle f^* + \boldsymbol{\delta}', \varphi(\mathbf{x}) \rangle \leq \|\boldsymbol{\delta}'\| \cdot \|\varphi(\mathbf{x})\| \leq \delta \cdot \|\varphi(\mathbf{x})\|. \tag{18}$$

Define $\boldsymbol{\Sigma}_f^+ := \mathbb{E}_+ [\sin \langle f, \varphi(\mathbf{x}) \rangle \varphi(\mathbf{x}) \otimes \varphi(\mathbf{x})]$ and $\hat{\boldsymbol{\Sigma}}_f^+$ as its empirical counterpart approximated using X_+ . We can see that $a = \langle \tilde{s}, [\boldsymbol{\Sigma}_{f^*}^+ - \hat{\boldsymbol{\Sigma}}_{\bar{f}}^+] \tilde{u} \rangle + \langle \tilde{s}, [\boldsymbol{\Sigma}_{f^*}^- - \hat{\boldsymbol{\Sigma}}_{\bar{f}}^-] \tilde{u} \rangle$. Moreover,

$$\begin{aligned}
\langle \tilde{s}, [\boldsymbol{\Sigma}_{f^*}^+ - \hat{\boldsymbol{\Sigma}}_{\bar{f}}^+] \tilde{u} \rangle &\stackrel{i}{\leq} \mathbb{E}_+ \{ \delta \cdot \|\varphi(\mathbf{x})\| \cdot \langle \tilde{s}, \varphi(\mathbf{x}) \otimes \varphi(\mathbf{x}) \tilde{u} \rangle \} \\
&\leq \delta \langle \tilde{u}, \mathbb{E}_+ \{ (\boldsymbol{\Sigma}_{f^*} + \lambda \mathbf{I})^{-1} \varphi(\mathbf{x}) \} \cdot \|\varphi(\mathbf{x})\| \rangle \cdot \|\tilde{u}\| \\
&\leq \delta \|\tilde{u}\| \cdot \|(\boldsymbol{\Sigma}_{f^*} + \lambda \mathbf{I})^{-1} \mathbb{E}_+ \varphi(\mathbf{x})\| \cdot \|\tilde{u}\|
\end{aligned}$$

(i) is due to (18). Following a similar line of reasoning, we can see

$$\langle \tilde{s}, [\boldsymbol{\Sigma}_{f^*}^- - \hat{\boldsymbol{\Sigma}}_{\bar{f}}^-] \tilde{u} \rangle \leq \delta \|(\boldsymbol{\Sigma}_{f^*} + \lambda \mathbf{I})^{-1} \mathbb{E}_- [\varphi(\mathbf{x})]\| \cdot \|\tilde{u}\|^2.$$

By setting $\delta \leq 4 \max \left(\|(\boldsymbol{\Sigma}_{f^*} + \lambda \mathbf{I})^{-1} \mathbb{E}_+ [\varphi(\mathbf{x})]\|, \|(\boldsymbol{\Sigma}_{f^*} + \lambda \mathbf{I})^{-1} \mathbb{E}_- [\varphi(\mathbf{x})]\| \right)^{-1}$, we have

$$a \leq \frac{\|\tilde{u}\|^2}{2}. \tag{19}$$

Now we inspect b . We can see $|b| \leq \left| \tilde{s} \hat{\boldsymbol{\Sigma}}_{\bar{f}}^+ \tilde{u} - \mathbb{E}_+ [\tilde{s} \hat{\boldsymbol{\Sigma}}_{\bar{f}}^+ \tilde{u}] \right| + \left| \tilde{s} \hat{\boldsymbol{\Sigma}}_{\bar{f}}^- \tilde{u} - \mathbb{E}_- [\tilde{s} \hat{\boldsymbol{\Sigma}}_{\bar{f}}^- \tilde{u}] \right|$. Define a scalar random variable

$$Z_f^{(i)} := \sin \langle f, \varphi(\mathbf{x}_i) \rangle \cdot \langle \tilde{s}, \varphi(\mathbf{x}_i) \otimes \varphi(\mathbf{x}_i) \tilde{u} \rangle.$$

By definition $\frac{1}{n_+} \sum_{i=1}^{n_+} Z_f^{(i)} = \tilde{s}^\top \hat{\boldsymbol{\Sigma}}_f^+ \tilde{u}$. Therefore

$$\left| \frac{1}{n_+} \sum_{i=1}^{n_+} Z_{\bar{f}}^{(i)} - \mathbb{E} Z_{\bar{f}} \right| \leq \sup_f \left| \frac{1}{n_+} \sum_{i=1}^{n_+} Z_f^{(i)} - \mathbb{E} Z_f \right|.$$

Since $0 \leq Z_f^{(i)} \leq \|\tilde{s}\| \cdot \|\tilde{u}\| \cdot \|\varphi(\mathbf{x})\|^2 \leq \|(\boldsymbol{\Sigma}_{f^*} + \lambda \mathbf{I})^{-1} \tilde{u}\| \|\tilde{u}\| \leq \frac{\|\tilde{u}\|^2}{\lambda}$, using Uniform Law of Large Number for bounded random variable (Theorem 4.10, Wainwright (2019)),

$$\sup_f \left| \frac{1}{n_+} \sum_{i=1}^{n_+} Z_f^{(i)} - \mathbb{E} Z_f \right| \leq 2\mathcal{R}_{n_+}(\mathcal{F}_Z) + \frac{\|\tilde{u}\|^2 \cdot \|\varphi(\mathbf{x})\|^2}{\lambda \sqrt{n_+}},$$

with high probability, where $\mathcal{R}_{n_+}(\mathcal{F}_Z)$ is the Rademacher complexity of the function class of Z_f . It remains to bound $\mathcal{R}_{n_+}(\mathcal{F}_Z)$. It can be seen that $Z_f = h[\langle f, \varphi(\mathbf{x}) \rangle]$ where h is a Lipschitz continuous function

with Lipschitz constant $\frac{\|\tilde{u}\|^2}{\lambda}$. Hence, due to Ledoux–Talagrand contraction inequality (see, e.g., (5.61) in Wainwright (2019)), $\mathcal{R}_{n_+}(\mathcal{F}_Z)$ is upperbounded by,

$$\mathcal{R}_{n_+}(\mathcal{F}_Z) \leq \frac{2\|\tilde{u}\|^2}{\lambda} \cdot \mathcal{R}_{n_+}(\mathcal{H}^*) \leq \frac{C_0 \cdot \|\tilde{u}\|^2}{\lambda\sqrt{n_+}},$$

where C_0 is a universal constant. The last inequality is due to Corollary 14.5 in Wainwright (2019). Therefore

$$\left| \tilde{s} \hat{\Sigma}_{\tilde{f}}^+ \tilde{u} - \mathbb{E}_+ \left[\tilde{s} \hat{\Sigma}_{\tilde{f}}^+ \tilde{u} \right] \right| \leq \frac{C_0 \cdot \|\tilde{u}\|^2}{\lambda\sqrt{n_+}} + \frac{\|\tilde{u}\|^2 \cdot \|\varphi(\mathbf{x})\|^2}{\lambda\sqrt{n_+}}$$

and similarly,

$$\left| \tilde{s} \hat{\Sigma}_{\tilde{f}}^- \tilde{u} - \mathbb{E}_- \left[\tilde{s} \hat{\Sigma}_{\tilde{f}}^- \tilde{u} \right] \right| \leq \frac{C_0 \cdot \|\tilde{u}\|^2}{\lambda\sqrt{n_-}} + \frac{\|\tilde{u}\|^2 \cdot \|\varphi(\mathbf{x})\|^2}{\lambda\sqrt{n_-}}.$$

Therefore,

$$|b| \leq \frac{C_0 \cdot \|\tilde{u}\|^2}{\lambda\sqrt{n_{\min}}} + \frac{\|\tilde{u}\|^2 \cdot \|\varphi(\mathbf{x})\|^2}{\lambda\sqrt{n_{\min}}}, \quad (20)$$

with high probability. Substituting (19) and (20) into (17), we get

$$\langle \tilde{s}^\top, -\nabla_f \ell(f^*) - \lambda f^* \rangle + \frac{\max(C_0, \|\varphi(\mathbf{x})\|^2) \cdot \|\tilde{u}\|^2}{\lambda\sqrt{n_{\min}}} \geq \|\tilde{u}\|^2 - \frac{1}{2} \|\tilde{u}\|^2.$$

Using triangle inequality and Hölder's inequality, we have

$$-\langle \tilde{s}, \nabla_f \ell(f^*) \rangle + \|\tilde{u}\| \|(\Sigma_{f^*} + \lambda \mathbf{I})^{-1} \lambda f^*\| + \frac{\max(C_0, 1) \|\tilde{u}\|^2}{\lambda\sqrt{n_{\min}}} \geq \frac{1}{2} \|\tilde{u}\|^2. \quad (21)$$

Due to Assumption 1, $\mathbb{E}[\nabla_f \ell(f^*)] = 0$. Hence,

$$\begin{aligned} -\langle \tilde{s}, \nabla_f \ell(f^*) \rangle &= -\langle \tilde{s}, \mathbb{E}[\nabla_f \ell(f^*)] \rangle - \langle \tilde{s}, \nabla_f \ell(f^*) - \mathbb{E}[\nabla_f \ell(f^*)] \rangle \\ &= 0 - \langle \tilde{s}, \nabla_f \ell(f^*) - \mathbb{E}[\nabla_f \ell(f^*)] \rangle. \end{aligned}$$

We can see

$$|\langle \tilde{s}, \nabla_f \ell(f^*) - \mathbb{E}[\nabla_f \ell(f^*)] \rangle| \leq \frac{\|\tilde{u}\|}{\lambda} \|\nabla_f \ell(f^*) - \mathbb{E}[\nabla_f \ell(f^*)]\| \leq \frac{C_1 \|\tilde{u}\|}{\lambda\sqrt{n_{\min}}} \quad (22)$$

holds with high probability and C_1 is a universal constant (due to Lemma 2).

Moreover, since $f^* \in \mathcal{R}(\Sigma_{f^*}^\beta)$, there exists $g \in \mathcal{H}$, $f^* = \Sigma_{f^*}^\beta g$. Notice Σ_{f^*} is a bounded, compact, self-adjoint linear operator (see Section E). Therefore, Hilbert-Schmidt Theorem indicates, $\Sigma_{f^*} = \sum_i \alpha_i \psi_i \langle \psi_i, \cdot \rangle$, where ψ_i, α_i are eigenfunctions and eigenvalues of Σ_{f^*} respectively. Hence,

$$\begin{aligned} \|(\Sigma_{f^*} + \lambda \mathbf{I})^{-1} f^* \lambda\| &= \|(\Sigma_{f^*} + \lambda \mathbf{I})^{-1} \Sigma_{f^*}^\beta g \lambda\| \leq \left\| \sum_i \langle \psi_i, g \rangle \psi_i \cdot \frac{\alpha_i^\beta \lambda}{\alpha_i + \lambda} \right\| \\ &\leq \lambda^\beta \left\| \sum_i \langle \psi_i, g \rangle \right\| \leq \|\Sigma^{*-\beta} f\| \cdot \lambda^\beta. \end{aligned} \quad (23)$$

Combine (21), (22) and (23) and cancel $\|\tilde{u}\|$, we can conclude that

$$\frac{C_1}{\lambda\sqrt{n_{\min}}} + \|\Sigma^{*-\beta} f\| \cdot \lambda^\beta + \frac{\max(C_0, \|\varphi(\mathbf{x})\|^2)}{\lambda\sqrt{n_{\min}}} \geq \frac{1}{2} \|\tilde{u}\|,$$

with high probability. Set $\lambda = \frac{\max(C_1, C_0, 1)}{n_{\min}^{1/4}}$, we have

$$\frac{2}{n_{\min}^{1/4}} + \frac{\max(C_1, C_0, 1)^\beta \|\Sigma^{*-\beta} f^*\|}{n_{\min}^{\beta/4}} \geq \frac{1}{2} \|\tilde{u}\|,$$

holds with high probability. Therefore, $\exists N_2$, when $n_{\min} > N_2$, $\|\tilde{u}\| = O_p(n_{\min}^{-\beta/4})$.

Since $\|\tilde{u}\| = o_p(1)$, as long as $\delta \geq K \cdot n_{\min}^{-\beta/4}$, $K > 0$ is a constant, there exists a constant N such that, when $n_{\min} > N$, \tilde{f} is in the interior of \mathcal{H}^* with high probability. When this happens, the constraint $f \in \mathcal{H}^*$ is no longer active. This means \tilde{f} is a stationary point of the objective function in (13). Moreover, $\tilde{f} \in \mathcal{H}^*$, so it is in the feasible region of (11) thanks to Assumption 2. This further indicates that \tilde{f} is also a solution to (11). As (11) is a strictly convex optimization problem, \tilde{f} is also its only solution. Therefore $\tilde{f} = \hat{f}$ and $\|\hat{f} - f^*\| = \|\tilde{f} - f^*\| = O_p(n_{\min}^{-\beta/4})$. \square

Lemma 2. *Given any $f^* \in \mathcal{H}$ such that $\mathbb{E}[\nabla_f \ell(f^*)] = 0$, if $\|\varphi(\mathbf{x})\|_{\mathcal{H}} \leq B$ then*

$$P(\|\nabla_f \ell(f^*)\|_{\mathcal{H}} > \delta) \leq 4 \exp\left(-\frac{n_{\min} \delta^2}{B^2}\right).$$

Proof. Write down the definition of $\nabla_f \ell(f^*)$. Notice

$$\nabla_f \ell(f^*) = \underbrace{-\frac{1}{n_+} \sum_{i=1}^{n_+} \cos\langle f, \varphi(\mathbf{x}_i) \rangle \varphi(\mathbf{x}_i)}_a + \underbrace{\frac{1}{n_-} \sum_{i=1}^{n_-} \sin\langle f, \varphi(\mathbf{x}_i) \rangle \varphi(\mathbf{x}_i)}_b.$$

By using Hilbert-space Hoeffding's inequality Rosasco et al. (2010), we know for all $\delta_a, \delta_b > 0$

$$P(\|a - \mathbb{E}[a]\|_{\mathcal{H}} > \delta_a) \leq 2 \exp\left(-\frac{C n_+ \delta_a^2}{B^2}\right) \text{ and } P(\|b - \mathbb{E}[b]\|_{\mathcal{H}} > \delta_b) \leq 2 \exp\left(-\frac{C n_- \delta_b^2}{B^2}\right),$$

where C is a constant. Let $\delta = \delta_a = \delta_b$,

$$\begin{aligned} P(\|a + b\|_{\mathcal{H}} > 2\delta) &= P(\|a + b - (\mathbb{E}[a] + \mathbb{E}[b])\|_{\mathcal{H}} > 2\delta) \\ &\leq P(\|a - \mathbb{E}[a]\|_{\mathcal{H}} + \|b - \mathbb{E}[b]\|_{\mathcal{H}} > \delta_a + \delta_b) \\ &\leq P(\|a - \mathbb{E}[a]\|_{\mathcal{H}} > \delta_a) + P(\|b - \mathbb{E}[b]\|_{\mathcal{H}} > \delta_b) \\ &\leq 4 \exp\left(-\frac{C n_{\min} \delta^2}{B^2}\right), \end{aligned}$$

where the first equality used the condition that $\mathbb{E}[\nabla_f \ell(f^*)] = \mathbb{E}[a] + \mathbb{E}[b] = 0$. This completes the proof. \square

C Proof of Proposition 6

Proof. We start from the definition of $\mathbb{E}[\nabla_f \ell(f^*)]$:

$$\begin{aligned} -\mathbb{E}[\nabla_f \ell(f^*)] &= \mathbb{E}_+ \left[\frac{1}{n_+} \sum_{i=1}^n \cos\langle f^*, \varphi(\mathbf{x}_i) \rangle \varphi(\mathbf{x}_i) \right] - \mathbb{E}_- \left[\frac{1}{n_-} \sum_{i=1}^n \sin\langle f^*, \varphi(\mathbf{x}_i) \rangle \varphi(\mathbf{x}_i) \right] \\ &= \mathbb{E}_+ [\cos\langle f^*, \varphi(\mathbf{x}) \rangle \varphi(\mathbf{x})] - \mathbb{E}_- \left[\frac{\sin\langle f^*, \varphi(\mathbf{x}) \rangle}{\cos\langle f^*, \varphi(\mathbf{x}) \rangle} \cos\langle f^*, \varphi(\mathbf{x}) \rangle \varphi(\mathbf{x}) \right] \\ &= \mathbb{E}_+ [\cos\langle f^*, \varphi(\mathbf{x}) \rangle \varphi(\mathbf{x})] - \mathbb{E}_- \left[\frac{p_+(\mathbf{x})}{p_-(\mathbf{x})} \cos\langle f^*, \varphi(\mathbf{x}) \rangle \varphi(\mathbf{x}) \right] \\ &= \mathbb{E}_+ [\cos\langle f^*, \varphi(\mathbf{x}) \rangle \varphi(\mathbf{x})] - \mathbb{E}_+ [\cos\langle f^*, \varphi(\mathbf{x}) \rangle \varphi(\mathbf{x})] = 0, \end{aligned}$$

where the third equality is due to the fact that $\langle f^* \varphi(\mathbf{x}) \rangle = \arctan \frac{p_+(\mathbf{x})}{p_-(\mathbf{x})}$. Since $p_+/p_- \in [0, \infty)$, $\langle f, \varphi(\mathbf{x}) \rangle \in [0, \pi/2)$. As f^* is unique by assumption, Assumption 1 holds. \square

D Derivation of Lagrangian Dual of (12)

In this section, we provide the derivation of the dual formulation (12). First, we rewrite the Lagrangian of (11) and add a bias term b^3 .

$$\begin{aligned} \hat{f} := & \operatorname{argmin}_{f \in \mathcal{H}, \mathbf{u} \in \mathbb{R}^{n_+ + n_-}, b} -\frac{1}{n_+} \sum_{i=1}^{n_+} \sin u_{i_+} - \frac{1}{n_-} \sum_{i=1}^{n_-} \cos u_{i_-} + \frac{\lambda}{2} \|f\|_{\mathcal{H}}^2, \\ \text{subject to: } & u_i \in [0, \frac{\pi}{2}], u_i = \langle f, \varphi(\mathbf{x}_i) \rangle + b, \forall i, \end{aligned} \quad (24)$$

where i_+ and i_- are defined as indices of positive and negative samples as mentioned in the main text.

Writing the Lagrangian of (24):

$$\begin{aligned} L(f, \mathbf{u}, \boldsymbol{\xi}, \boldsymbol{\xi}', \boldsymbol{\alpha}) = & -\frac{1}{n_+} \sum_{i=1}^{n_+} \sin u_{i_+} - \frac{1}{n_-} \sum_{i=1}^{n_-} \cos u_{i_-} + \sum_{i=1}^{n_+ + n_-} \alpha_i u_i - \sum_{i=1}^{n_+ + n_-} \alpha_i \langle f, \varphi(\mathbf{x}_i) \rangle \\ & - \sum_{i=1}^{n_+ + n_-} \alpha_i b - \sum_{i=1}^{n_+ + n_-} \xi_i u_i + \sum_{i=1}^{n_+ + n_-} \xi'_i u_i - \frac{\pi}{2} \sum_{i=1}^{n_+ + n_-} \xi'_i + \frac{\lambda}{2} \|f\|_{\mathcal{H}}^2. \end{aligned}$$

By setting $\nabla_f L(f, \mathbf{u}, \boldsymbol{\xi}, \boldsymbol{\xi}', \boldsymbol{\alpha}) = 0$, we obtain $f = \frac{1}{2\lambda} \sum_{i=1}^{n_+ + n_-} \alpha_i \varphi(\mathbf{x}_i)$.

By setting $\nabla_b L(f, \mathbf{u}, \boldsymbol{\xi}, \boldsymbol{\xi}', \boldsymbol{\alpha}) = 0$, we obtain $0 = \sum_{i=1}^{n_+ + n_-} \alpha_i$.

By setting $\nabla_{\mathbf{u}_+} L(f, \mathbf{u}, \boldsymbol{\xi}, \boldsymbol{\xi}', \boldsymbol{\alpha}) = \mathbf{0}$, we obtain, $\mathbf{u}_+ = \arccos [n_+(-\boldsymbol{\xi}_+ + \boldsymbol{\xi}'_+ + \boldsymbol{\alpha}_+)]$.

By setting $\nabla_{\mathbf{u}_-} L(f, \mathbf{u}, \boldsymbol{\xi}, \boldsymbol{\xi}', \boldsymbol{\alpha}) = \mathbf{0}$, we obtain, $\mathbf{u}_- = \arcsin [n_-(\boldsymbol{\xi}_- - \boldsymbol{\xi}'_- - \boldsymbol{\alpha}_-)]$.

Substituting expressions for f , \mathbf{u}_+ , \mathbf{u}_- and $\boldsymbol{\alpha}$ into $L(f, \mathbf{u}, \boldsymbol{\xi}, \boldsymbol{\xi}', \boldsymbol{\alpha})$ and collecting terms, we obtain

$$\begin{aligned} L'(\boldsymbol{\xi}, \boldsymbol{\xi}', \boldsymbol{\alpha}) = & -\frac{1}{n_+} \sum_{i=1}^{n_+} \sin \arccos [n_+(-\xi_{i_+} + \xi'_{i_+} + \alpha_{i_+})] \\ & - \frac{1}{n_-} \sum_{i=1}^{n_-} \cos \arcsin [n_-(\xi_{i_-} - \xi'_{i_-} - \alpha_{i_-})] \\ & + \sum_{i=1}^{n_+} (-\xi_{i_+} + \xi'_{i_+} + \alpha_{i_+}) \arccos [n_+(-\xi_{i_+} + \xi'_{i_+} + \alpha_{i_+})] \\ & - \sum_{i=1}^{n_-} (\xi_{i_-} - \xi'_{i_-} - \alpha_{i_-}) \arcsin [n_-(\xi_{i_-} - \xi'_{i_-} - \alpha_{i_-})] \\ & - \frac{\pi}{2} \sum_{i=1}^{n_+ + n_-} \xi'_i - \frac{1}{4\lambda} \boldsymbol{\alpha}^\top \mathbf{K} \boldsymbol{\alpha}, \end{aligned}$$

where \mathbf{K} is the kernel matrix computed on the dataset $X_+ \cup X_-$. Then the dual problem becomes:

$$\begin{aligned} & \max_{\boldsymbol{\alpha}, \boldsymbol{\xi} \geq \mathbf{0}, \boldsymbol{\xi}' \geq \mathbf{0}} L'(\boldsymbol{\xi}, \boldsymbol{\xi}', \boldsymbol{\alpha}), \\ \text{subject to: } & n_+(-\xi_{i_+} + \xi'_{i_+} + \alpha_{i_+}) \in [0, 1], n_-(\xi_{i_-} - \xi'_{i_-} - \alpha_{i_-}) \in [0, 1], \forall i_+, i_-. \end{aligned} \quad (25)$$

Note $\sin(\arccos(y)) = \cos(\arcsin(y)) = \sqrt{1-y^2}$. By setting $t_i = n_+(-\xi_{i_+} + \xi'_{i_+} + \alpha_{i_+})$ and $t'_i = -n_-(\xi_{i_-} - \xi'_{i_-} - \alpha_{i_-})$, we can verify (25) is the same as (12).

³In the main text, we did not include the bias term b for conveniences of theoretical analysis. However, in actual computation, we need the bias term.

E Properties of Operator Σ_{f_0}

By construction, it is easy to verify that Σ_{f_0} is self-adjoint.

First, we prove that the integral operator

$$\Sigma_{f_0} u = \mathbb{E}_+[\sin\langle f_0, \varphi(\mathbf{x}) \rangle \varphi(\mathbf{x}) \cdot u(\mathbf{x})] + \mathbb{E}_-[\cos\langle f_0, \varphi(\mathbf{x}) \rangle \varphi(\mathbf{x}) \cdot u(\mathbf{x})],$$

is a bounded operator. For all $u \in \text{Ball}(0, 1)$, where $\text{Ball}(0, 1)$ is the unit ball in \mathcal{H} ,

$$\begin{aligned} \|\Sigma_{f_0} u\|_{\mathcal{H}} &\leq \|\mathbb{E}_+[\sin\langle f_0, \varphi(\mathbf{x}) \rangle \varphi(\mathbf{x}) \cdot u(\mathbf{x})]\|_{\mathcal{H}} + \|\mathbb{E}_-[\cos\langle f_0, \varphi(\mathbf{x}) \rangle \varphi(\mathbf{x}) \cdot u(\mathbf{x})]\|_{\mathcal{H}} \\ &\leq \mathbb{E}_+[\|\sin\langle f_0, \varphi(\mathbf{x}) \rangle \varphi(\mathbf{x})\|_{\mathcal{H}} \cdot \|u(\mathbf{x})\|_{\mathcal{H}}] + \mathbb{E}_-[\|\cos\langle f_0, \varphi(\mathbf{x}) \rangle \varphi(\mathbf{x})\|_{\mathcal{H}} \cdot \|u(\mathbf{x})\|_{\mathcal{H}}] \\ &\leq \mathbb{E}_+[\|\varphi(\mathbf{x})\|_{\mathcal{H}} \cdot \|u(\mathbf{x})\|_{\mathcal{H}}] + \mathbb{E}_-[\|\varphi(\mathbf{x})\|_{\mathcal{H}} \cdot \|u(\mathbf{x})\|_{\mathcal{H}}] \\ &\leq \mathbb{E}_+[\|\varphi(\mathbf{x})\|_{\mathcal{H}}] + \mathbb{E}_-[\|\varphi(\mathbf{x})\|_{\mathcal{H}}]. \end{aligned}$$

Hence, Σ_{f_0} is a bounded operator as long as $\|\varphi(\mathbf{x})\|_{\mathcal{H}}$ is bounded.

Second, we show Σ_{f_0} is trace class hence compact. Let $\psi_i, i \in \mathbb{N}$ be an orthonormal basis in \mathcal{H} , then

$$\begin{aligned} &\sum_i \langle \psi_i, \Sigma_{f_0} \psi_i \rangle \\ &= \mathbb{E}_+[\sin\langle f_0, \varphi(\mathbf{x}) \rangle \sum_{i \in \mathbb{N}} \langle \psi_i, \varphi(\mathbf{x}) \otimes \varphi(\mathbf{x}) \psi_i \rangle] + \mathbb{E}_-[\cos\langle f_0, \varphi(\mathbf{x}) \rangle \sum_{i \in \mathbb{N}} \langle \psi_i, \varphi(\mathbf{x}) \otimes \varphi(\mathbf{x}) \psi_i \rangle] \\ &= \mathbb{E}_+[\sin\langle f_0, \varphi(\mathbf{x}) \rangle \sum_{i \in \mathbb{N}} \langle \psi_i, \varphi(\mathbf{x}) \rangle^2] + \mathbb{E}_-[\cos\langle f_0, \varphi(\mathbf{x}) \rangle \sum_{i \in \mathbb{N}} \langle \psi_i, \varphi(\mathbf{x}) \rangle^2] \\ &= \mathbb{E}_+[\sin\langle f_0, \varphi(\mathbf{x}) \rangle \cdot \|\varphi(\mathbf{x})\|_{\mathcal{H}}^2] + \mathbb{E}_-[\cos\langle f_0, \varphi(\mathbf{x}) \rangle \cdot \|\varphi(\mathbf{x})\|_{\mathcal{H}}^2] < \infty \end{aligned}$$

holds as long as $\|\varphi(\mathbf{x})\|_{\mathcal{H}}$ is bounded. This shows Σ_{f_0} is trace-class and therefore, compact.

F Hyperparameter Tuning

In our numerical simulations, we consider the following three density ratio estimators:

- logistic regression density ratio estimator Gutmann and Hirayama (2012),
- log-linear Kullback Leibler Importance Estimation Procedure (KLIEP) (Section 5.22, Sugiyama et al. (2012)) and
- the proposed approach, using the dual formulation (12).

Since logistic regression and log-linear KLIEP estimators are unconstrained optimizations, kernel methods can be easily employed using Representer Theorem (Theorem 4.2, Scholkopf and Smola (2001)).

In all three methods, we use Gaussian kernel whose bandwidth is chosen from the following list of candidates: $\sigma_0 \cdot [0.2, 1.15, 2.1, 3.05, 4]$, where σ_0 is the median value of the pairwise distance of data points. The ‘‘median heuristic’’ has been widely used in two-sample kernel methods, such as Gretton et al. (2012).

For logistic regression and the proposed approach, the regularization parameter is chosen from

$$[0.000000100, 0.000005623, 0.000316228, 0.017782794, 1].$$

For KLIEP, the regularization parameter is chosen from

$$[0.001000000, 0.005623413, 0.031622777, 0.177827941, 1],$$

as any regularization parameter smaller than 0.001 will result numerical errors in KLIEP optimization.

The optimal pair of regularization parameter and kernel bandwidth is chosen by using 5-fold cross validation. Fully runnable code is included in the supplementary material (in the ‘‘code’’ folder) and we invite reviewers to reproduce and verify our results.

References

- D. M. Blei, A. Kucukelbir, and J. D. McAuliffe. Variational inference: A review for statisticians. *Journal of the American Statistical Association*, 112(518):859–877, 2017.
- D. C Edwards and C. E. Metz. A utility-based performance metric for roc analysis of n -class classification tasks. In *Medical Imaging 2007: Image Perception, Observer Performance, and Technology Assessment*, volume 6515, pages 21 – 30. SPIE, 2007.
- D. C. Edwards and C. E Metz. Optimality of a utility-based performance metric for roc analysis. In *Medical Imaging 2008: Image Perception, Observer Performance, and Technology Assessment*, volume 6917, pages 122 – 127. SPIE, 2008.
- S. Eguchi and J. Copas. A class of logistic-type discriminant functions. *Biometrika*, 89(1):1–22, 2002.
- C. Ferri, J. Hernández-Orallo, and M. A. Salido. Volume under the roc surface for multi-class problems. In *Machine Learning: European Conference of Machine Learning 2003*, pages 108–120, 2003.
- K. Fukumizu. *Exponential manifold by reproducing kernel Hilbert spaces*, page 291–306. Cambridge University Press, 2009.
- K. Fukumizu, L. Song, and A. Gretton. Kernel bayes’ rule: Bayesian inference with positive definite kernels. *The Journal of Machine Learning Research*, 14(1):3753–3783, 2013.
- D. J. Goodenough, K. Rossmann, and L. B Lusted. Radiographic applications of receiver operating characteristic (roc) curves. *Radiology*, 110(1):89–95, 1974.
- I. Goodfellow, J. Pouget-Abadie, M. Mirza, B. Xu, D. Warde-Farley, S. Ozair, A. Courville, and Y. Bengio. Generative adversarial nets. In *Advances in neural information processing systems 27*, pages 2672–2680, 2014.
- D. M. Green and J. A. Swets. *Signal detection theory and psychophysics*, volume 1. Wiley New York, 1966.
- A. Gretton, K. M. Borgwardt, M. J. Rasch, B. Schölkopf, and A. Smola. A kernel two-sample test. *Journal of Machine Learning Research*, 13(Mar):723–773, 2012.
- M. Gutmann and J. Hirayama. Bregman divergence as general framework to estimate unnormalized statistical models. In *In Proceedings of the Conference on Uncertainty in Artificial Intelligence (UAI)*, page 283–290. AUAI Press, 2012.
- J. Hermans, V. Begy, and G. Louppe. Likelihood-free mcmc with amortized approximate ratio estimators. In *International Conference on Machine Learning*, pages 4239–4248. PMLR, 2020.
- S. Hido, Y. Tsuboi, H. Kashima, M. Sugiyama, and T. Kanamori. Statistical outlier detection using direct density ratio estimation. *Knowledge and information systems*, 26(2):309–336, 2011.
- J.B. Hiriart-Urruty and C. Lemaréchal. *Fundamentals of convex analysis*. Springer Science & Business Media, 2004.
- B. Kim, S. Liu, and M. Kolar. Two-sample inference for high-dimensional markov networks. *Journal of the Royal Statistical Society: Series B (Statistical Methodology)*, 2021. doi: <https://doi.org/10.1111/rssb.12446>.
- S. Kullback and R. A. Leibler. On information and sufficiency. *Annals of Mathematical Statistics*, 22:79–86, 1951.
- Z. Lin, A. Khetan, G. Fanti, and S. Oh. Pacgan: The power of two samples in generative adversarial networks. In *In Proceedings of the Advances in Neural Information Processing Systems (NeurIPS), 2018*, volume 31, 2018.

- S. Liu, M. Yamada, N. Collier, and M. Sugiyama. Change-point detection in time-series data by relative density-ratio estimation. *Neural Networks*, 43:72–83, 2013.
- L. B. Lusted. Signal detectability and medical decision-making. *Science*, 171(3977):1217–1219, 1971.
- X. Nguyen, M. J. Wainwright, and M. I. Jordan. On surrogate loss functions and f-divergences. *The Annals of Statistics*, 37(2):876–904, 2009.
- X. Nguyen, M. J. Wainwright, and M. I. Jordan. Estimating divergence functionals and the likelihood ratio by convex risk minimization. *IEEE Transactions on Information Theory*, 56(11):5847–5861, 2010.
- S. Nowozin, B. Cseke, and R. Tomioka. f-gan: Training generative neural samplers using variational divergence minimization. In *Advances in Neural Information Processing Systems 29*, pages 271–279, 2016.
- G. Peyre and M. Cuturi. Computational optimal transport. *Foundations and Trends in Machine Learning*, 11(5-6):355–607, 2019.
- Mark D. Reid and Robert C. Williamson. Information, divergence and risk for binary experiments. *Journal of Machine Learning Research*, 12(22):731–817, 2011.
- L. Rosasco, M. Belkin, and E. De Vito. On learning with integral operators. *Journal of Machine Learning Research*, 11(2), 2010.
- B. Scholkopf and A. J. Smola. *Learning with kernels: support vector machines, regularization, optimization, and beyond*. MIT press, 2001.
- B. Sriperumbudur, K. Fukumizu, A. Gretton, A. Hyvärinen, and R. Kumar. Density estimation in infinite dimensional exponential families. *Journal of Machine Learning Research*, 18(57):1–59, 2017.
- B. K. Sriperumbudur, K. Fukumizu, A. Gretton, B. Schölkopf, and G. RG Lanckriet. On the empirical estimation of integral probability metrics. *Electronic Journal of Statistics*, 6:1550–1599, 2012.
- I. Steinwart, D. R. Hush, and C. Scovel. Optimal rates for regularized least squares regression. In *Proceedings of Conference on Learning Theory (COLT) 2009*, pages 79–93, 2009.
- M. Sugiyama, T. Suzuki, and T. Kanamori. *Density Ratio Estimation in Machine Learning*. Cambridge University Press, 2012.
- M. J. Wainwright. *High-Dimensional Statistics: A Non-Asymptotic Viewpoint*. Cambridge University Press, 2019.